Romanian Reports in Physics, Vol. 63, No. 2, P. 394–400, 2011

SEARCH FOR EXOTIC PARTICLES WITH THE ANTARES DETECTOR*

GABRIELA EMILIA PĂVĂLAŞ*

Institute for Space Sciences, Atomistilor 409, PO Box Mg-23, Magurele, Ro 077125, Ilfov, Romania, e-mail: gpavalas@spacescience.ro

Received January 20, 2010

Abstract. Besides the detection of high energy neutrinos, the ANTARES telescope offers an opportunity to improve sensitivity to exotic particles. In this report we discuss the sensitivity of the ANTARES detector to slow nuclearites.

Key words: undersea neutrino telescopes, nuclearites.

1. INTRODUCTION

The primary goal of the ANTARES experiment is to observe high energy cosmic neutrinos through the detection of the Cherenkov light produced by up-going induced muons. The ANTARES detector may be also an excellent instrument to search for super heavy exotic particles like nuclearites [1, 2].

Nuclearites are hypothetical nuggets of strange quark matter that could be present in cosmic radiation. Their origin is related to energetic astrophysical phenomena (supernovae, collapsing binary strange stars, etc.). Down-going nuclearites could reach the ANTARES depth with velocities of ~ 300 km/s, emitting blackbody radiation at visible wavelengths while traversing the sea water.

2. THE ANTARES DETECTOR

The ANTARES detector has reached its nominal configuration in May 2008. Its 884 Optical Modules (OMs) are deployed on 12 vertical lines in the Western Mediterranean, at depths between 2050 and 2400 meters.

The OMs, consisting of a glass sphere housing a 10" Hamamatsu photomultiplier tube (PMT) [3], are arranged by triplet per storey. Each detector

---

* On behalf of the ANTARES Collaboration.

* Paper presented at the Annual Scientific Session of Faculty of Physics, University of Bucharest, June 5, 2009, Bucharest – Măgurele, Romania.

line, made of 25 storeys, is connected via interlinks to a Junction Box, itself connected to the shore station at La Seyne-sur-Mer through a 40 km long electro-optical cable. The strategy of the ANTARES data acquisition is based on the "all-data-to-shore" concept [4]. This implementation leads to the transmission of all raw data above a given threshold to shore, where different software triggers are applied for filtering before storage.

For the analysis presented here, only one trigger logic has been considered, that is based on local coincidences. A local coincidence (first level "L1" trigger) is defined either as a combination of two hits on two OMs of the same storey within 20 ns, or as a single hit with a large amplitude, typically 3 photoelectrons. The directional trigger requires five local coincidences anywhere in the detector causally connected, within a time window of 2.2 μs. When an event is triggered, all PMT pulses are recorded over 2.2 μs.

The ANTARES observatory was build gradually, giving rise to various detector layouts used for physics analysis. The 5-line, 10-line and 12-line detector configurations took data from January 2007, from December 2007 and from May 2008, respectively.

3. NUCLEARITES

Heavy nuggets of strange quark matter ($M \geq 10^{10}$ GeV), known as nuclearites, would be electrically neutral; the small positive electric charge of the quark core would be neutralized by electrons forming an electronic cloud or found in week equilibrium inside the core. The relevant energy loss mechanism is represented by the elastic collisions with the atoms of the traversed media, as shown in [5]:

$$\frac{\mathrm{d}E}{\mathrm{d}x} = -\sigma\rho v^2, \tag{1}$$

where ρ is the density of the medium, v is the nuclearite velocity and σ its geometrical cross section:

$$\sigma = \begin{cases} \pi(3M / 4\pi\rho_N)^{2/3} & \text{for } M \geq 8.4\times10^{14} \text{ GeV;} \\ \pi\times10^{-16}\,\text{cm}^2 & \text{for smaller masses,} \end{cases}$$

with $\rho_N \approx 3.6\times10^{14}$ g cm^{-3}. The mass limit in the above equation corresponds to a radius of the strange quark matter of 1 Å. Assuming a nuclearite of mass M enters the atmosphere with an initial (non-relativistic) velocity v, after crossing a depth L it will be slowed down to

$$v(L) = v_0 e^{-\frac{\sigma}{M}\int_0^L \rho_a \mathrm{d}x}, \tag{2}$$

where ρ_a is the air density at different depths. Considering the parameterization of the standard atmosphere from [6]:

$$\rho_a(h) = a\mathrm{e}^{-\frac{h}{b}} = a\mathrm{e}^{-\frac{H-L}{b}}, \tag{3}$$

where $a = 1.2\times10^{-3}$ g cm^{-3} and $b \approx 8.57\times10^{5}$ cm, $H \approx 50$ km is the total height of the atmosphere. The integral in Eq. 2 may be solved analytically.

The propagation of nuclearites in sea water is described also by Eq. 2, assuming ρ_a = 1 g cm^{-3} and substituting v_0 with the speed value at the Earth surface. Nuclearites moving into the water could be detected trough the black-body radiation emitted by the expanding cylindrical thermal shock wave [5]. The luminous efficiency (defined as the fraction of dissipated energy appearing as light) was estimated, in the case of water, to be $\eta \approx 3\times10^{-5}$ [5]. The number of visible photons emitted per unit path length can be computed as:

$$\frac{\mathrm{d}N_\gamma}{\mathrm{d}x} = \eta\frac{\mathrm{d}E/\mathrm{d}x}{\pi[eV]}, \tag{4}$$

assuming the average energy of visible photons π eV. The best present limit for a flux of down-going nuclearites was established by the MACRO experiment, at Gran Sasso [7].

4. SEARCH STRATEGY AND RESULTS

The Monte Carlo simulation of nuclearite detection in ANTARES assumes only the down-going part of an isotropic flux of nuclearites and an initial velocity (before entering the atmosphere) of $\beta = 10^{-3}$. A typical nuclearite event would cross the ANTARES detector in a characteristic time of ~ 1 ms, producing a luminosity that would exceed that of muons by several orders of magnitude. Down-going atmospheric muons represent the main background for nuclearite events. This analysis considers the 5-line ANTARES configuration.

Nuclearite events were simulated for masses of 3×10^{16} GeV, 10^{17} GeV and 10^{18} GeV, considering as simulation volume a hemisphere with a radius of 548 m that surrounds the 5-line detector. The initial point of the trajectory and the direction of the nuclearite are randomly generated. The algorithm proceeds in steps of 2 ns, evaluating the position and velocity of nuclearite at each iteration, as well as the number of hits on the optical modules of the detector.

The atmospheric muons were generated with a Monte Carlo code [8], that uses a dedicated parameterization of the flux of atmospheric muons and an energy range from 20 GeV to 500 TeV.

The data set used in this analysis covers 84 days of data acquisition with the 5-line detector.

Both simulated nuclearite and muon events have been processed with the directional trigger, that operated during the 5-line data acquisition. The directional trigger selects events having at least 5 L1 hits correlated in time. At this step, the background was added from a run taken in July 2007, at a baseline rate of 63.5 kHz. The lower detectable nuclearite mass in the 5-line configuration is about 3×10^{16} GeV.

The algorithm of the directional trigger selects from all the hits produced by a nuclearite only those that comply to the signal of a relativistic muon. These hits can be contained in a single snapshot or multiple snaphots for a single nuclearite event. Because nuclearites are slowly moving particles, multiple snapshots belonging to a single nuclearite event may span into intervals from hundreds of μs up to ~ 1ms. The multiplicity of snapshots for the simulated nuclearite events, selected by the directional trigger (268 events for 3×10^{16} GeV, 1706 for 10^{17} GeV and 319 for 10^{18} GeV), is presented in Fig. 1.

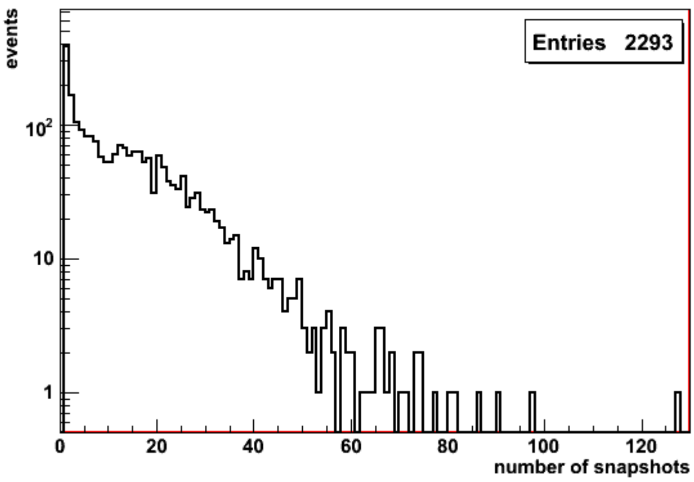

Fig. 1 – Snapshot distribution obtained for simulated nuclearite events with masses 3×10^{16}, 10^{17}, 10^{18} GeV, selected by the directional trigger.

The parameters studied in our analysis comprised the number of L1 triggered hits (see Section 2), the number of single hits (L0 hits, defined as hits with a threshold greater than 0.3 photoelectrons), the duration of the snapshot (defined as the time difference between the last and the first L1 triggered hits of the event) and the total amplitude of hits in the event, where a snapshot contains all PMT pulses related to a triggered muon event, usually in a time window of ~ 4 μs. The simulated events were comparated with data from an experimental run.

The majority of the snapshots produced by nuclearites from the studied sample are of short duration (< 500 ns), see Fig. 2. Longer snapshots (up to tens of μs) are also present, due to the large light output of events with masses $\geq 10^{17}$ Gev.

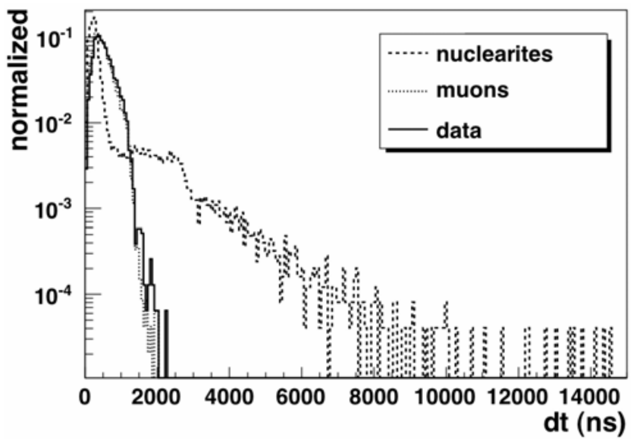

Fig. 2 – Normalized distributions as a function of the duration of snapshot for simulated nuclearites (dashed line), muons (dotted line) and data (continuous line).

Snapshots of nuclearites passing through the detector would also be characterized by a larger number of single hits than for atmospheric muons, as shown in Fig. 3.

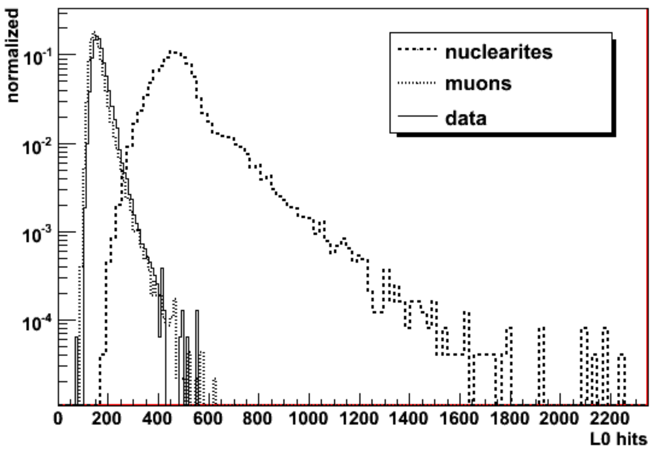

Fig. 3 – Normalized distributions of the number of L0 hits for simulated nuclearite (dashed line) and muon (dotted line) events and experimental data (continuous line).

A reasonable agreement is obtained between the distributions of simulated muons and data.

A possible selection criteria for nuclearite signal was obtained considering only the data sample as background. The distributions for data and simulated nuclearite events in the 2-dimensional plot L1 triggered hits *vs* L0 single hits show a clear separation, that was optimized using the linear cut presented in Fig. 4.

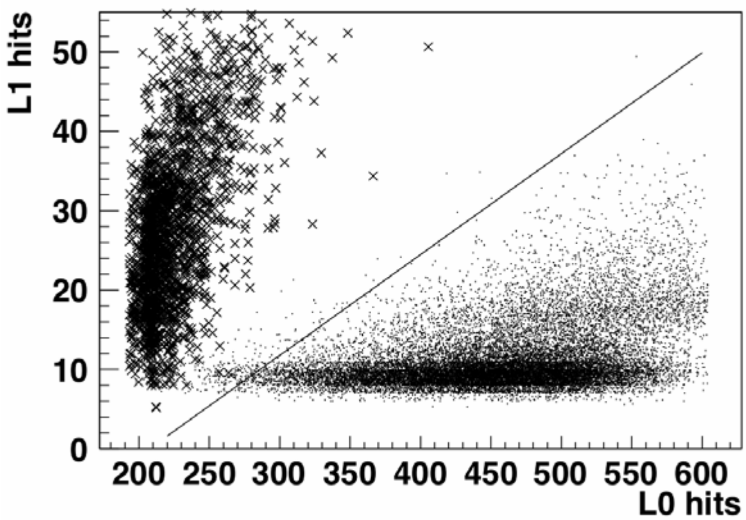

Fig. 4 – Muon data (crosses) and simulated nuclearite events (points) in a L1 triggered hits *vs*. L0 single hits plot. The points represent the corresponding values per snapshot. The linear cut was optimized for signal selection.

The linear cut has been applied to an extended data set, corresponding to 84 days of data acquisition in 5-line configuration. The data sample is reduced by 99.998%. A second cut has been applied to the remaining events, by requiring the multiple snapshot signatures within a time interval of 1 ms, characteristic to the crossing time of the detector by a nuclearite event. Three "events" with two snapshots each have passed the second cut.

The percentage of simulated nuclearite events remained after applying the cuts is given in Table 1. The triggered events below the linear cut are characterized by a low number of L1 hits and a large number of 0 single hits.

Table 1

Number of triggered simulated nuclearite events and percentage of events remaining after applying the cuts

Nuclearite mass (GeV)	Triggered events	Linear cut	Multiple snapshot cut
3×10^{16}	268	72.5%	16.3%
1×10^{17}	1706	96.8%	89.1%
1×10^{18}	319	98.7%	96.2%

The sensitivity of the ANTARES detector in 5-line configuration to a nuclearite flux was calculated according to Feldman-Cousins [9], considering a background of 3 events and no nuclearite event detected, for 84 active days of the detector, as shown in Fig. 5. The upper flux limit for nuclearite events with masses $\geq 10^{17}$ GeV is of the order of $\sim 10^{-16}$ cm^{-2} s^{-1} sr^{-1}.

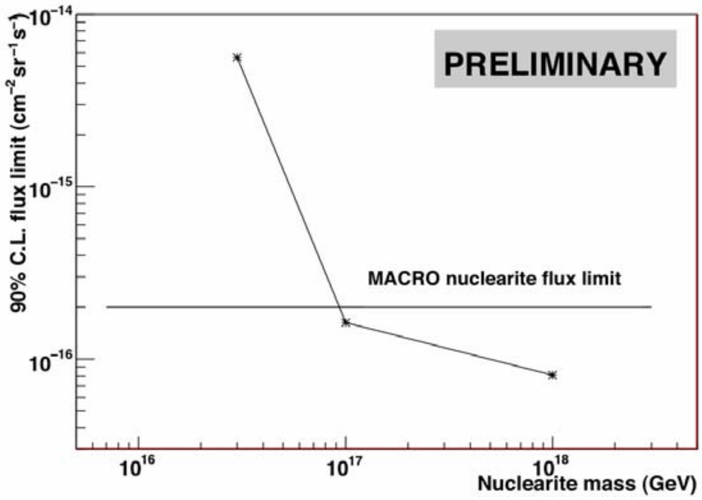

Fig. 5 – Sensitivity of the ANTARES detector in the 5-line configuration to a nuclearite flux, using 84 days of data taking.

5. CONCLUSIONS

This report presents a search strategy and a preliminary result of the expected sensitivity for non-relativistic nuclearites with the ANTARES detector in 5-line configuration. The sensitivity for nuclearites can be improved by using data taken in ANTARES nominal configuration and a less stringent trigger than directional trigger. The possibility of implementation in the data acquisition program of a trigger that uses the characteristics of nuclearite events in order to keep all data sent to shore for a time interval of about 20 ms is currently investigated.

Acknowledgements. The author acknowledges the colleagues from the ANTARES Collaborations for their many contributions and very fruitful discussions.

REFERENCES

1. V., Popa, Nucl. Instrum. Meth., **A567**, 480 (2006).
2. G., Pavalas, N., Picot-Clemente, Proceedings of the 31st ICRC, Lodz 2009, arXiv: 0908.0860.
3. J. A., Aguilar et al. (ANTARES Collaboration), Nucl. Instrum. Meth., **A555**, 132 (2005).
4. J. A., Aguilar et al. (ANTARES Collaboration), Nucl. Instrum. Meth., **A570**, 107 (2007).
5. A., De Rujula, S.L., Glashow, Nature, **312**, 734 (1984).
6. T., Shibata, Prog. Theor. Phys., **57**, 882 (1977).
7. M., Ambrosio et al. (MACRO Collaboration), Eur. Phys. J., **C26**, 163 (2002);
   G., Giacomelli and L., Patrizii, hep-ex/0506014.
8. G., Carminati et al., Computer Physics Communications, **179**, 915 (2008).
9. G.J., Feldman, R.D., Cousins, Physical Review, **D57**, 3873 (1998).